Proton-Proton Scattering at 970 MeV

D. V. BUGG, A. J. OXLEY,* J. A. ZOLL, J. G. RUSHBROOKE,* AND V. E. BARNES†
Cavendish Laboratory, Cambridge, England

AND

J. B. KINSON,‡ W. P. DODD, G. A. DORAN, AND L. RIDDIFORD
Department of Physics, The University, Birmingham, England

(Received 29 August 1963)

Proton-proton scattering has been studied at 970 MeV using the Birmingham University 1-BeV synchrotron and a 9-in.-diam liquid-hydrogen bubble chamber; 3945 events have been analyzed and cross sections determined for the various reactions. The elastic scattering cross section of 24.8±0.9 mb is significantly higher than the result of Dowell *et al.* using counters. The two experiments agree on the shape of the angular distribution, but not on its normalization; possible reasons for this are discussed. The elastic scattering angular distribution is peaked strongly forward, but does not agree quantitively with pure diffraction. Polarization effects observed in the elastic scattering agree with previous and more accurate counter experiments. Inelastic scattering is strongly influenced by the $(\frac{3}{2},\frac{3}{2})$ π^+p resonance and the peripheral mechanism. Theoretical predictions based on the single-pion exchange model are compared in detail with the experimental results and good quantitative agreement is obtained for small momentum transfers, particularly for the reaction $p+p \rightarrow n+p+\pi^+$. Even for small momentum transfers, asymmetries in the Treiman-Yang test and departure from the expected $(1+3\cos^2\theta)$ π^+-P angular distribution indicate that other mechanisms may be important. The cross section for double-pion production at 970 MeV is less than 0.2 mb.

1. INTRODUCTION

THE general picture of nucleon-nucleon interactions in the BeV region has become clear from a number of experiments using both visual and counter techniques.[1–4] The dominant inelastic interaction appears to be pion production via the formation of the well-known $(\frac{3}{2},\frac{3}{2})$ isobar, and previous results have shown striking agreement with the isobar model of Lindenbaum and Sternheimer.[2] Elastic scattering has been shown to be in qualitative agreement with pure diffraction scattering, although quantative discrepancies have led to speculation on the possible existence of a real part in the nucleon-nucleon potential[3,4] at these energies.

Both proton-proton and proton-neutron scattering have previously been studied at 1 BeV by Batson *et al.* using a diffusion cloud chamber.[5] A further investigation[6] with better statistics and greater accuracy using a liquid-hydrogen bubble chamber has now been completed. This paper reports on the measurement of 3945 proton-proton scattering events, and a subsequent paper will describe about 1800 pion production events in a neutron beam. Studies of neutron-neutron and proton-neutron scattering are being made with deuterium in the bubble chamber.

The proton-proton scattering events described in this paper come from two bubble chamber runs; 1073 from the first run were measured at Birmingham, and 2872 from the second at Cambridge. Selection and identification of events, measurements, and analysis have been carried out independently in the two laboratories. Both groups have used semiautomatic measuring machines and digital computers. Any significant differences of technique are described below, but the final results from the two groups agree sufficiently well, so that they may with confidence be combined to increase the statistical accuracy.

2. EXPERIMENTAL ARRANGEMENT

The full energy circulating beam of the proton synchrotron was allowed to strike a carbon target, and protons scattered at 4° were accepted by the collimation system. The fringing field of the synchrotron provided adequate momentum analysis of the beam, which was collimated vertically and horizontally to about ½° before entering the bubble chamber. The beam energy of 970±15 MeV is calculated from the known properties of the synchrotron field, allowing for energy loss in the bubble chamber and vacuum tank walls, and the synchrotron target assembly. Measurements on the opening angles of proton-proton elastic scattering events near 90° center-of-mass confirm this figure within the measurement accuracy of ±25 MeV. The energy

---

* Present address: Department of Nuclear Physics, University of Oxford, Oxford, England.

† Present address: The Brookhaven National Laboratory, Upton, New York.

‡ Present address: the Track Chamber Division, CERN, Geneva, Switzerland.

[1] An extensive list of references is given by W. J. Fickinger, E. Pickup, D. K. Robinson, and E. O. Salant, Phys. Rev. **125**, 2082 (1962); Phys. Rev. Letters **7**, 196 (1961).

[2] S. J. Lindenbaum and R. M. Sternheimer, Phys. Rev. **105**, 1874 (1957).

[3] W. M. Preston, R. Wilson, and J. C. Street, Phys. Rev. **118**, 579 (1960).

[4] B. Cork, W. A. Wenzel, and C. W. Causey, Phys. Rev. **107**, 859 (1957).

[5] A. P. Batson, B. B. Culwick, J. G. Hill, and L. Riddiford, Proc. Roy. Soc. (London) **A251**, 218 (1959); A. P. Batson, B. B. Culwick, H. B. Klepp, and L. Riddiford, *ibid.* **A251**, 233 (1959).

[6] V. E. Barnes, D. V. Bugg, W. P. Dodd, J. B. Kinson, and L. Riddiford, Phys. Rev. Letters **7**, 288 (1961).

spread of particles in a similar beam has been measured by counters to be ±10 MeV.

The Birmingham liquid-hydrogen bubble chamber, 9 in. in diameter and 4 in. deep, has been described previously.[7] It was operated in a pulsed magnetic field of 15 kG; the field varied by less than 2% over the chamber volume, and from pulse to pulse. Events in the chamber were photographed on three stereo views. The chamber was run at as low a temperature as was compatible with reasonable track quality, so that bubble density measurements could be used to distinguish pions from protons.

3. ANALYSIS AND CROSS SECTIONS

All frames were scanned twice, using a different view for each scan. This was necessary to achieve a high scanning efficiency for elastic scatters through small angles. The scanning was done on a table which could be tipped to allow the scanner to look along the beam at a shallow angle, thus, foreshortening the picture and making small angle scatters conspicuous. It was found that the scanning efficiency was better than 99.5% for events in which the proton scattered through laboratory angles greater than 6°, even in a plane perpendicular to the camera plane. For smaller angles than this, there was some loss of events in planes unfavorably oriented relative to the cameras.

The events were measured on the semiautomatic measuring machines Cul-de-Sac[8] at Birmingham, and Tara I[9] at Cambridge. Both machines had a measuring accuracy of about 5 μ on the film. Subsequent geometrical reconstruction and kinematic analysis of the events was conventional.[10] Errors on the measured quantities were deduced directly from the known measuring accuracy and the length and orientation of the track, with due allowance for distortion, energy loss, and multiple scattering in the liquid hydrogen. It was found that the error in momentum measurements was typically 10%. Range measurements were used wherever possible; the density of the liquid hydrogen was deduced from π-μ-e decays to be 0.0595 g/cc.

Owing to the narrow angular collimation of the beam, most events due to tracks other than beam particles could be rejected at the scanning table. A further check was made by the computer that the incident track of every event was parallel to the beam direction within the errors of measurement. Only events within a restricted fiducial region were processed, the limit set by the computer being slightly tighter than that set by the scanners so as to obviate any possible scanning biases.

At Cambridge, all events were put through a GUTS[11]-type fitting program and values of χ^2, the statistical estimate of the goodness of fit, were used as a guide to the identification of events. A rather simpler kinematics program was used at Birmingham. Fits were attempted first to the hypotheses

$$p+p \rightarrow p+p, \tag{1}$$

$$p+p \rightarrow d+\pi^+, \tag{2}$$

and

$$p+p \rightarrow \pi^++d. \tag{2a}$$

Events of these types were immediately distinguishable from inelastic reactions, largely because of the requirements of coplanarity of the three tracks and correlation between scattering angles, but sometimes also by curvature or range measurements. It is worth noting, however, that (1) is not kinematically distinguishable from (2) in a small angular region around center-of-mass scattering angles $\cos\theta=0.84$ for (1), and (correspondingly) $\cos\theta=0.34$ for (2). In this region, however, bubble density clearly distinguishes slow protons from pions.

All events clearly inelastic, or not fitting the above hypotheses well, or having the wrong bubble densities, were fitted to the hypotheses

$$p+p \rightarrow p+\pi^++n, \tag{3}$$

$$p+p \rightarrow \pi^++p+n, \tag{3a}$$

$$p+p \rightarrow p+p+\pi^0, \tag{4}$$

$$p+p \rightarrow d+\pi^++\pi^0, \tag{5}$$

or

$$p+p \rightarrow \pi^++d+\pi^0. \tag{5a}$$

Frequently, an event would fit more than one hypothesis kinematically, but there was rarely any difficulty in assigning the identification on the basis of bubble densities. In many cases, however, it was kinematically impossible to exclude the presence of an extra π^0, but since only three definite examples of double-pion production were observed, the number of double-pion production events mistakenly classified as (3) or (4) is likely to be much less than the statistical fluctuation within each class.

Separation of events of types (1) and (2) from the rest was feasible throughout a larger region of the chamber than separation of the inelastic modes (3) to (5). At Cambridge, the larger region was used for a study of elastic scattering and the determination of the elastic/inelastic ratio, while a smaller region was used to study inelastic scattering. At Birmingham, the fiducial region used was the same for all events. The number of elastic events, corrected for scanning losses at small angles, as described in Sec. 4, was 2160, while the corresponding number of inelastic events was 1955.

[7] D. C. Colley, J. B. Kinson, and L. Riddiford, Nucl. Instr. Methods 4, 26 (1959).
[8] B. B. Culwick and S. J. Goldsack, Nucl. Instr. Methods 13, 118 (1961).
[9] O. R. Frisch and A. J. Oxley, Nucl. Instr. Methods 9, 92 (1960).
[10] D. V. Bugg, Ph.D. thesis, University of Cambridge, 1961 (unpublished); J. B. Kinson, Ph.D. thesis, University of Birmingham, 1961 (unpublished).
[11] J. P. Berge, F. T. Solmitz, and H. D. Taft, Rev. Sci. Instr. 32, 538 (1961).

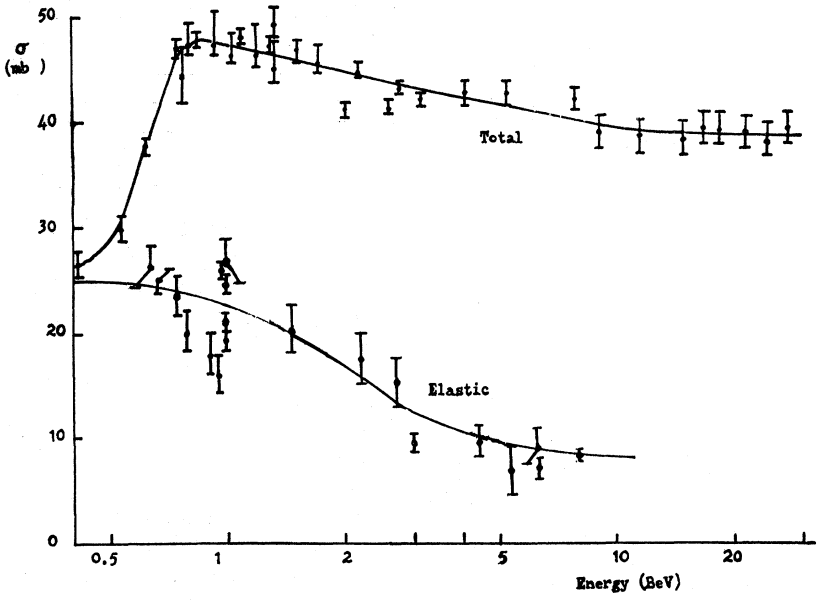

FIG. 1. Elastic and total p-p cross-sections as a function of energy. The results not mentioned in the text are taken from: F. F. Chen, C. P. Leavitt, and A M. Shapiro, Phys. Rev. **103**, 211 (1956); M. J. Longo, J. A. Helland, W. N. Hess, B. J. Moyer, V. Perez-Mendez, Phys. Rev. Letters **3**, 568 (1959); A. Ashmore, G. Cocconi, A. N. Diddens, and A. M. Wetherell, *ibid.* **5**, 576 (1960); G. Von Dardel, D. H. Frisch, R. Mermod, R. H. Milburn, P. A. Piroue, M. Vivargent, G. Weber, and K. Winter, *ibid.* **5**, 333 (1960); T. N. Morris, E. C. Fowler, and J. D. Garrison, Phys. Rev. **103**, 1472 (1956); L. W. Smith, A. W. McReynolds, and G. Snow, Phys. Rev. **97**, 1186 (1955); P. J. Duke, W. O. Lock, P. V. March, W. M. Gibson, J. G. McEwen, I. S. Hughes, and H. Muirhead, Phil. Mag. **2**, 204 (1957); B. Cork, W. A. Wenzel, and C. W. Causey, Phys. Rev. **107**, 859 (1957); R. W. Wright, G. Saphir, W. M. Powell, G. Maenchen, and W. B. Fowler, *ibid.* **105**, 1413 (1957); R. M. Kalbach, J. J. Lord, and C. H. Tsao, Phys. Rev. **113**, 325 (1959); V. B. Lyubimov, P. K. Markov, E. N. Tsyganov, Cheng P'U-Ying, and M. G. Shafranov, Zh. Eksperim. i Teor. Fiz. **37**, 910 (1959) [English transl.: Soviet Phys.—JETP **10**, 651 (1960)].

Figure 1 has been compiled from the many counter and chamber experiments in the BeV region, and, by interpolation, a total cross section of 47.3 ± 1.0 mb is estimated at 970 MeV. Using this to normalize cross sections, the total elastic cross section at 970 MeV is 24.8 ± 0.9 mb. This result, together with others at 1 BeV and other energies, is also shown in Fig. 1.

Cross sections for the various reactions are shown in Table I. The numbers of events of types (1) and (2) are those in the larger fiducial region, corrected for scanning losses. The numbers of types (3) and (4) are those from the smaller region, subsequently used to study these reactions in detail; scanning losses were negligible for inelastic events.

4. ELASTIC SCATTERING

As a result of being scattered at 4° from the carbon target, the beam was believed[12] to be approximately 30% polarized with the spin direction vertical in the chamber. Since the chamber has horizontal windows, the spin direction $\boldsymbol{\sigma}$ pointed towards the cameras. Let ϕ (similar to ϕ in Fig. 8) be the azimuthal angle between this spin direction and the normal $\mathbf{n}$ to the plane of the event, the normal being up if the fast proton went to the right. Let θ be the center-of-mass scattering angle.

[12] C. J. Batty and S. J. Goldsack, Proc. Phys. Soc. (London) **A70**, 165 (1957); R. J. Homer, W. K. McFarlane, A. W. O'Dell, E. J. Sacharidis, and G. H. Eaton, Nuovo Cimento **23**, 690 (1962).

After two scans, the scanning efficiency was better than 99.5% for elastic scattering in the interval $0<\cos\theta<0.965$. Some scanning losses occurred in the interval $0.965<\cos\theta<0.985$; however, by restricting the polarization analysis to azimuthal angles such that $|\cos\phi|>0.5$ (i.e., to events close to the horizontal plane in the chamber), it was possible to avoid any bias at the expense of a loss in statistics. For the smallest scattering angles, such that $0.985<\cos\theta$, it was not possible to correct reliably for scanning losses; these events correspond to recoil proton tracks less than 5 mm long. The distribution of events between horizontal and vertical planes may be gauged by the average value of

TABLE I. Cross sections for p-p scattering at 970 MeV. The numbers of events for reactions (1) and (2) refer to a larger fiducial region.

	Reaction	No. of events	Cross section (mb)
(1)	$p+p\rightarrow p+p$	2160	$24.8\ \pm0.9$
(2)	$p+p\rightarrow d+\pi^+$	42	0.48 ± 0.08
(3)	$p+p\rightarrow p+n+\pi^+$	1414	$18.3\ \pm0.7$
(4)	$p+p\rightarrow p+p+\pi^0$	285	$3.7\ \pm0.3$
(5)	$p+p\rightarrow p+p+\pi^++\pi^-$	1	—
(6)	$p+p\rightarrow p+n+\pi^++\pi^0$	1	—
(7)	$p+p\rightarrow d+\pi^++\pi^0$	1	—
(8)	$p+p\rightarrow p+n+\pi^+$ or $p+p+\pi^0$	8	—

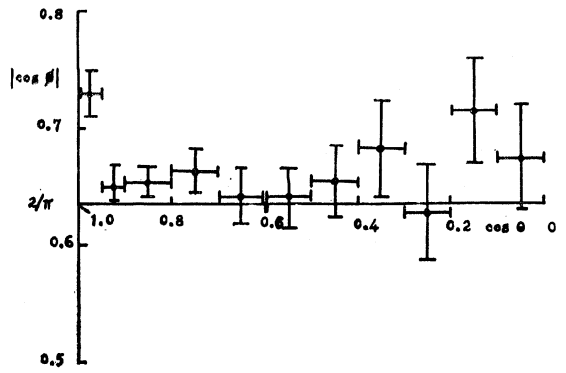

FIG. 2. The distribution of elastic events between horizontal and vertical planes.

$|\cos\phi|$. This quantity is plotted in Fig. 2 as a function of the center-of-mass scattering angle. It should be $2/\pi$ if there is no bias, and larger if there is a bias towards finding horizontal events. It is clear from Fig. 2 that no significant bias exists except for $\cos\theta>0.95$, although most points are slightly above $2/\pi$.

The angular distribution is shown in Fig. 3. It is peaked strongly forward, as one would expect if the process is one of diffraction. The scanning loss in the region $\cos\theta>0.985$ is a difficulty in evaluating the total elastic cross section. However, if it is assumed that there is no real part to the forward scattering amplitude, and that the scattering is not spin-dependent, then, from the optical theorem,

$$\frac{d\sigma}{d\Omega}(0^\circ)=|\mathrm{Im}f(0)|^2=\left(\frac{k}{4\pi}\sigma_T\right)^2=16.8\ \mathrm{mb/sr}, \quad (6)$$

where k is the wave number and σ_T is the total cross section. In this event, it is estimated that there would be 139 events in the region $\cos\theta>0.985$, and the total elastic cross section σ_E is 24.8 ± 0.9 mb. If, as seems possible from the discussion below, the cross section at 0° is larger than this, the value of σ_E must be increased by $(0.092)\{(d\sigma/d\Omega)(0^\circ)-16.8\}$mb.

This value of σ_E is in disagreement with the result of 20.8 ± 1.0 mb obtained by Dowell *et al.*[13] using counters (Fig. 1). They determined relative cross sections at angles in the region $0.95>\cos\theta>0$, extrapolated to $\cos\theta=1$, and normalized their results to the figure of 16.3 mb/sr obtained from Eq. (6) using $\sigma_T=46.1$ mb. This extrapolation was based on powers of $\cos\theta$ up to $\cos^6\theta$, and might have been affected by neglect of higher powers. Equally plausible is that the cross section at 0° may be greater than 16.8 mb/sr. An absolute measurement of the differential cross section has recently been made using counters by McFarlane *et al.*[14] They obtain an elastic cross section of 26.8 ± 2.3 mb (Fig. 1) and a forward scattering cross section of 21.4 ± 0.5 mb/sr.

The optical theorem strictly applies only to each spin substate separately.[15] If the total cross section is different in the singlet and triplet states, then

$$\sigma_T=\tfrac{1}{4}\sigma_s+\tfrac{3}{4}\sigma_t,$$

where σ_s and σ_t are the cross sections in pure singlet and triplet states, respectively. It is readily demonstrated that $(d\sigma/d\Omega)(0^\circ)$ takes its smallest value if $\sigma_s=\sigma_t$. Any spin dependence of the total cross section will cause $(d\sigma/d\Omega)(0^\circ)$ to be greater than the value given by Eq. (6). At 3 BeV, Preston Wilson, and Street[3] have observed that $(d\sigma/d\Omega)(0^\circ)$ is 10% above the value deduced from Eq. (6), while $\mathrm{Re}(0)<0.1\ \mathrm{Im}(0)$. At 1 BeV, large polarization effects have been observed in the elastic scattering[16] and, thus, it is plausible to expect spin dependence of the total cross section.

If the results of Dowell *et al.* are renormalized to $\sigma_E=24.8$ mb, they are in good agreement with the results of this experiment, as can be seen in Fig. 3. When

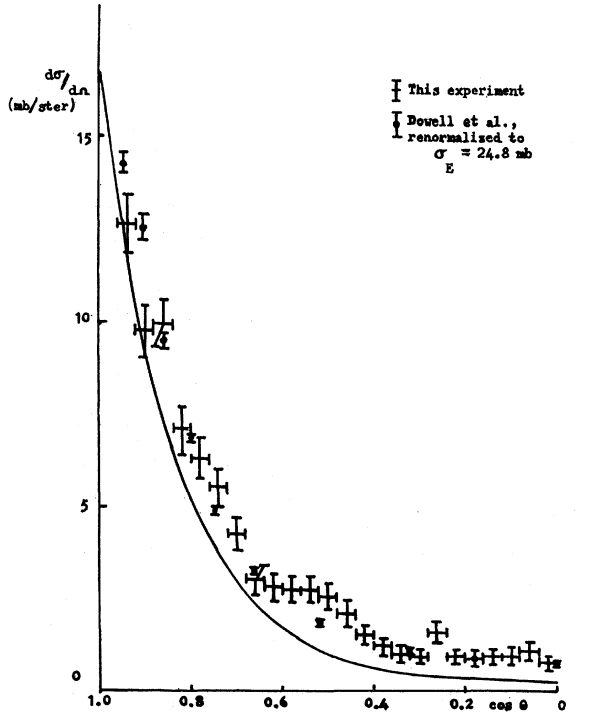

FIG. 3. The elastic scattering angular distribution. The results of this experiment are at 970 MeV, and those of Dowell *et al.* at 1010 MeV. The full line shows the distribution deduced from Eqs. (7) and (8) for pure diffraction at 970 MeV.

[13] J. D. Dowell, W. R. Frisken, G. Martelli, B. Musgrave, H. B. Van der Raay, and R. Rubinstein, Nuovo Cimento **18**, 818 (1960).

[14] W. K. McFarlane, R. J. Homer, A. W. O'Dell, E. J. Sacharidis, and G. H. Eaton, University of Birmingham, Preprint No. 13, 1962 (unpublished).

[15] J. Hamilton, *The Theory of Elementary Particles* (Clarendon Press, Oxford, 1959), p. 14; D. Blokhintsev, Zh. Eksperim. i Teor. Fiz. **39**, 1152 (1960) [English transl.: Soviet Phys.—JETP **12**, 802 (1961)].

[16] R. J. Homer, G. W. Hutchinson, W. K. McFarlane, A. W. O'Dell, R. Rubinstein, and E. J. Sacharidis, Nuovo Cimento **16**, 1132 (1960).

extrapolated to 0°, they would predict a cross section of 19.5 mb/sr in the forward direction.

It has frequently been suggested[4,5] that elastic p-p scattering in the BeV region is pure diffraction, and that the scattering amplitude should, therefore, be of the form

$$f(\theta)=iRJ_1(KR\sin\theta)/\sin\theta,$$

where J_1 is the first-order Bessel function, and R is the radius of the absorbing nucleon causing the diffraction. Such a form, however, can, at best, describe singlet states, since it is symmetric in $\cos\theta$.

The correct form of the scattering amplitude, according to the Kirchoff diffraction theory,[17] is

$$f(\theta)=\frac{iRJ_1(KR\sin\theta)}{\sin\theta}\cdot\frac{(1+\cos\theta)}{2}.$$

Then remembering that the final state contains two identical particles,

$$\frac{d\sigma}{d\Omega}=\tfrac{3}{4}|f(\theta)-f(\pi-\theta)|^2+\tfrac{1}{4}|f(\theta)+f(\pi-\theta)|^2$$
$$=\frac{R^2(1-\frac{3}{4}\sin^2\theta)}{\sin^2\theta}\cdot J_1^2(KR\sin\theta). \quad (7)$$

Such a formula cannot be exact, since when integrated it results in an elastic cross section less than πR^2. However, one would hope that it applied for small values of θ. Taking the value of $R=0.88$ F from

$$\sigma_T=2\pi R^2, \quad (8)$$

the angular distribution is given by the solid line on Fig. 3. Agreement with experiment is poor, even at quite small angles, but would be improved if scattering were stronger in the singlet than in the triplet state.

5. POLARIZATION IN ELASTIC SCATTERING

If the beam has a polarization P_1 when scattered out of the synchrotron and if the polarization at a second scatter is P_2, then the azimuthal distribution of the scattering planes of elastic events will be

$$d^2\sigma/d\theta d\phi\propto 1+P_1P_2(\theta)\cos\phi. \quad (9)$$

P_2 is a function of the center-of-mass scattering angle θ, and gives some indication of the angular momentum waves contributing to the scattering.

Using only those events with $|\cos\phi|>0.5$, values of P_1P_2 have been determined for intervals of $\cos\theta$ of 0.1, and are shown in Fig. 4(a). Although limited by statistics, they are of the same sign and general form as the counter results of Homer *et al.*,[12,16] shown for comparison in Fig. 4(b). Both experiments seem to indicate a maximum polarization at about $\cos\theta=0.5$ or 0.6.

[17] A. Sommerfeld, *Optics* (Academic Press Inc., New York, 1954), p. 197 et seq.; R. W. Ditchburn, *Light* (Blackie & Son Ltd., London, 1952), p. 152 et seq.

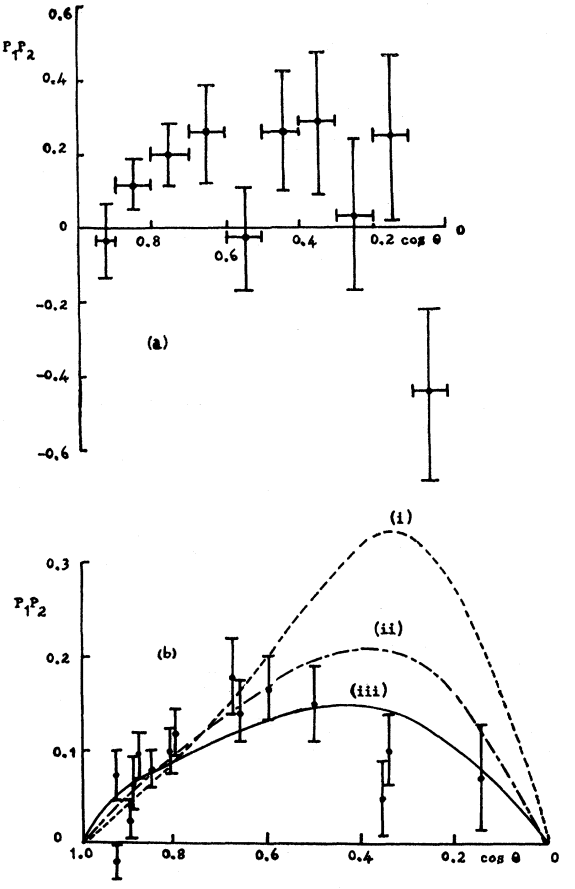

FIG. 4. The left-right asymmetry, P_1P_2, as a function of center of-mass scattering angle, observed (a) in this experiment, (b) by Homer *et al.* using counters. The three curves show values of P_1P_2 calculated from (i) P_1P_2 $(d\sigma/d\Omega)=0.37\sin\theta\cos\theta$ mb/sr, (ii) $P_1P_2(d\sigma/d\Omega)=0.19\sin\theta\cos\theta(1+2.17\cos^2\theta)$mb/sr, and (iii) $P_1P_2(d\sigma/d\Omega)=0.19\sin\theta\cos\theta(1+1.5\cos^2\theta+1.5\cos^4\theta)$mb/sr.

Contributions to the polarization arise only from triplet states, so that it takes the form[18]

$$P_2(\theta)(d\sigma/d\Omega)=\sin\theta\cos\theta[A+B\cos^2\theta+C\cos^4\theta+\cdots]. \quad (10)$$

The strong forward peak of the angular distribution makes it difficult to produce a polarization maximum at values of $\cos\theta$ as large as 0.5 without invoking the term with coefficient C, i.e., without the use of F waves or significant interference terms between P and H waves. This is illustrated in Fig. 4(b) by least-squares fits to the data of increasing order in $\cos\theta$; contributions from terms of the order $\cos^5\theta$ or higher are required to explain the large polarization near the forward direction, implying a long-range spin-dependent force at this energy.

6. THE REACTION $p+p\rightarrow d+\pi^+$

The 42 events of this type correspond to a cross section of 0.48 ± 0.08 mb. This result is higher than that

[18] L. Wolfenstein, Ann. Rev. Nucl. Sci. 6, 43 (1956).

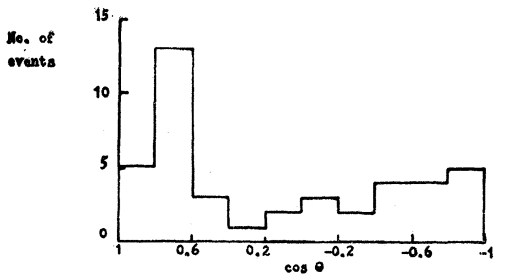

FIG. 5. The angular distribution of deuterons from the reaction $p+p \rightarrow d+\pi^+$.

obtained previously by Batson *et al.*[5] using a diffusion cloud chamber, but is in good agreement with the value of about 0.5 mb predicted by Mandelstam[19] on the basis of a modified isobar model, in which it is assumed that the pion resonates with one of the nucleons in the deuteron.

The angular distribution of the 42 events is shown in Fig. 5. Here the angle θ is the center-of-mass angle between the incident proton and the deuteron direction in the final state. The angular distribution should be symmetrical backward and forward; it is consistent with $(C+\cos^2\theta)$, the form predicted by Mandelstam on the assumption that only S and P waves are effective between nucleon and isobar in the intermediate state.

There are far too few events to look for polarization effects; the azimuthal distribution shows no marked asymmetry.

7. INELASTIC SCATTERING

The absence of appreciable double-pion production at this energy is striking. Only seven four-prong events were observed within the fiducial region, and of these six were examples of $p+p \rightarrow p+p+e^++e^-+\gamma$, with one example of $p+p \rightarrow p+p+\pi^++\pi^-$. In addition, one event of the type $p+p \rightarrow p+n+\pi^++\pi^0$ was positively identified, but the accuracy of measurement was such that the possibility of an extra π^0 in reactions (3) and (4) could not be excluded in many cases. If double-pion production is governed purely by statistical considerations, evaluation of the relevant Clebsch-Gordan coefficients shows that the reactions:

$$p+p \rightarrow p+p+\pi^0+\pi^0,$$
$$p+p \rightarrow p+n+\pi^++\pi^0,$$
$$p+p \rightarrow p+p+\pi^++\pi^-,$$

and

$$p+p \rightarrow n+n+\pi^++\pi^+,$$

should be in the ratio 2:9:6:3. Events classified into reactions (3) and (4) in Table I are, therefore, unlikely to be appreciably contaminated with cases of double-

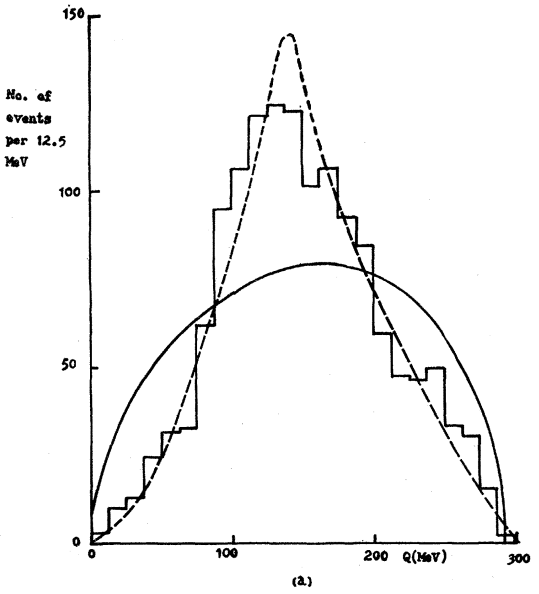

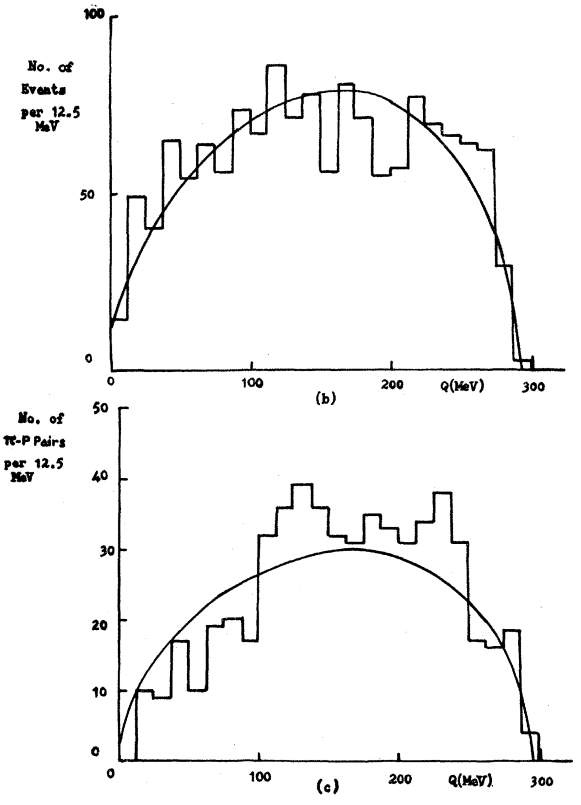

FIG. 6. Q-value distributions of (a) π^+p pairs and (b) π^+n pairs from $p+p \rightarrow p+n+\pi^+$, and (c) πp^0 pairs from $p+p \rightarrow p+p+\pi^0$. $Q=\omega-M-\mu$. The solid curves are the phase-space predictions, and the dashed curve the isobar model prediction, normalized to the total number of events.

[19] S. Mandelstam, Proc. Roy. Soc. (London) **A244**, 491 (1958).

pion production, and it is probably safe to say that the total cross section for double-pion production at this energy is less than 0.2 mb. The sole example of reaction (7) was an event in which the deuteron was clearly identified by its simultaneous high momentum and bubble density, and also by the kinematics.

There have been three popular models for describing inelastic scattering in the range of energies which includes that of this experiment. The oldest and simplest is the Fermi statistical model,[20] which pictures the scattering as an interaction so strong that thermodynamic equilibrium is reached among all possible states, with the result that the final state is governed entirely by phase-space factors. This theory was soon shown to be inconsistent with experiment by Yuan and Lindenbaum,[21] who found the center-of-mass energy distributions of positive and negative pions produced in hydrogen and beryllium by 1.0- and 2.3-BeV protons to be strongly peaked at about 150 MeV, which is just the center-of-mass energy at the $(\frac{3}{2},\frac{3}{2})$ resonance in π-p scattering. This phenomenon is well illustrated in the present experiment by the Q-value distributions shown in Figs. 6(a), (b), and (c) of $p\pi^+$ and $n\pi^+$ pairs from reaction (3) and $p\pi^0$ pairs from reaction (4); the solid curves are phase-space predictions.

The isobar model of Lindenbaum and Sternheimer,[2] based on this observation, regards single meson production as a two-stage process, e.g., $p+p\rightarrow I^{++}+n$, $I^{++}\rightarrow p+\pi^+$, where I^{++} is the $(\frac{3}{2},\frac{3}{2})$ resonant state. Quantitatively, the model suggests that the cross section for production of any particular final state is the two-body phase-space factor for production of I^{++} and n, multiplied by the cross section for π^+-p scattering at the energy of this pair in their own center-of-mass system. The isobar is usually assumed to be produced isotropically and also to decay isotropically in its own rest system. The dashed curve in Fig. 6(a) is for this model. It has been quite successful in describing single-pion production in π-p and p-p scattering.

The third model is the "Spectator" model of Chew and Low.[22] The original proposal of Chew and Low was a field theoretical statement of the possibility of extrapolating from the physical region to a pole in the region of negative kinetic energy for the recoil particle. Many authors[23] have since applied the model to the physical region. Taking p-p scattering as a specific example, all authors concentrate on the Feynman diagrams of Fig. 7. Diagram (b) is obtained from (a) by interchanging the nucleons in the initial state, and (c) and (d) are obtained from (a) and (b) by interchanging the nucleons in the final state. Four-momenta are used to label the particles, q_2 referring to the neutron and q_1 to the proton

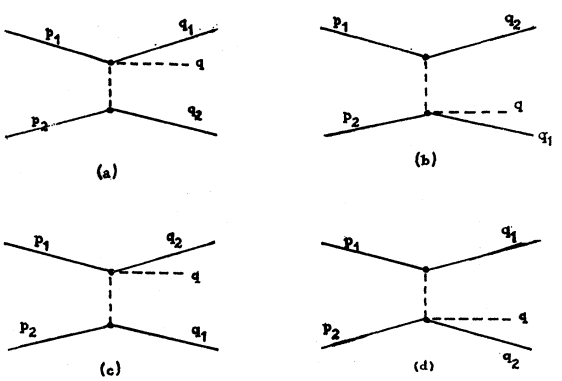

FIG. 7. The Feynman diagrams considered in peripheral nucleon-nucleon interactions.

in the $pn\pi^+$ final state. Figure 7(a) is redrawn in Fig. 8 in the laboratory system, taking p_1 at rest.

These diagrams may be discussed[24] in terms of five independent Lorentz invariants formed from the four-momenta of the five particles. However, it is convenient to analyze the reaction in terms of two Lorentz invariants and three angles. Consider Fig. 7(a). The invariants are

$$\Delta^2=(p_2-q_2)^2, \tag{11}$$

and

$$\omega^2=-(q+q_1)^2. \tag{12}$$

Δ is the 4-momentum transfer between the incident proton and the neutron, and ω is the total energy of the pion and proton of the final state in their own center-of-mass system. The angles are θ, the scattering angle of the pion in the πp rest system, i.e., the angle between $\mathbf{q}$ and $(\mathbf{p}_2-\mathbf{q}_2)$ in the πp rest system; χ, the angle between the normals $\mathbf{q}\times\mathbf{q}_1$ and $\mathbf{q}_2\times\mathbf{p}_2$ to the planes of the πp system and the incident proton and scattered neutron, respectively; and ϕ, the angle between the normal $\mathbf{q}_2\times\mathbf{p}_2$ and the spin direction of the incident proton.

Chew and Low point out that, although other diagrams will contribute to the scattering, those of Fig. 7

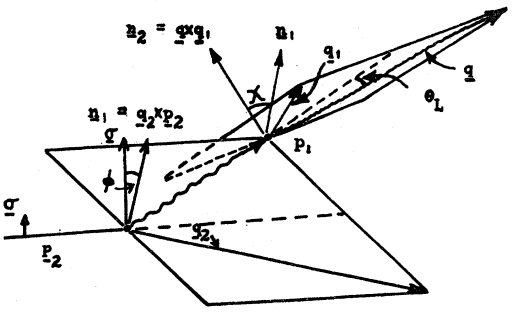

FIG. 8. The scattering as seen in the laboratory, with definitions of the angles ϕ and χ. θ is obtained from θ_L by a Lorentz transformation along the direction of the intermediate pion to the π^+p rest system; the normals are unaffected by this transformation.

[20] E. Fermi, Progr. Theoret. Phys. (Kyoto) **5**, 570 (1950).
[21] L. C. L. Yuan and S. J. Lindenbaum, Phys. Rev. **103**, 404 (1956).
[22] G. F. Chew and F. E. Low, Phys. Rev. **113**, 1640 (1959).
[23] See, for example, E. Ferrari and F. Selleri, Suppl. Nuovo Cimento **24**, 453 (1962), which also gives many other references.
[24] G. Da Prato, Nuovo Cimento **22**, 123 (1961); E. Ferrari and F. Selleri, *ibid.* **27**, 1450 (1963).

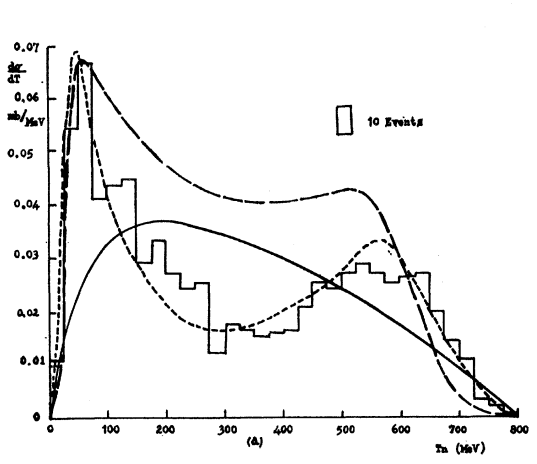

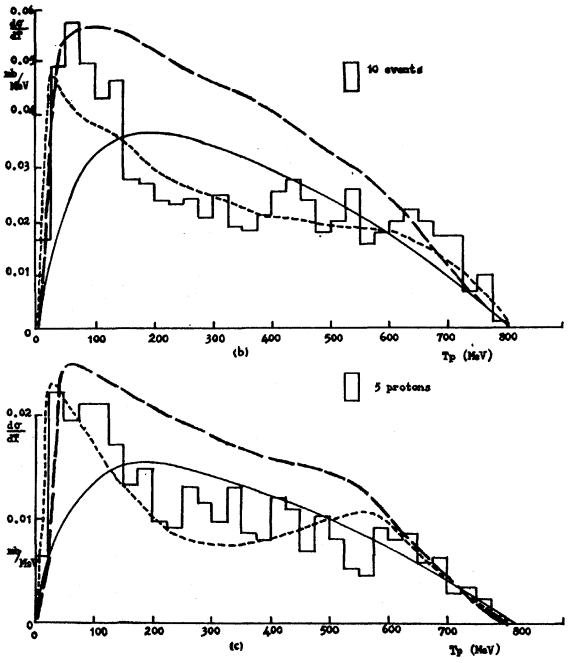

FIG. 9. Laboratory energy spectra of (a) neutrons and (b) protons from $p+p \rightarrow p+n+\pi^+$, and (c) protons from $p+p \rightarrow p+p+\pi^0$. The solid curves are phase-space predictions normalized to the total number of events, and the dotted and dashed curve are the absolute predictions of the peripheral model with and without (Ref. 24) the pionic form factor.

have a pole in the scattering amplitude which is closer to the physical region than that of any other diagram, namely, when $\Delta^2=-\mu^2$, where μ is the pion mass. At this pole, the proton p_2 acts simply as a source of real pions, from which the other proton scatters elastically. In the physical region, the intermediate pion is virtual (i.e., its mass squared is equal to $-\Delta^2$, which is no longer μ^2), and its momentum spectrum is governed by the factor

$$K(\Delta^2)=\Delta^2/(\Delta^2+\mu^2)^2. \tag{13}$$

Selleri[25] has shown that Fig. 7(a) by itself would be responsible for a cross section

$$\frac{\partial^2\sigma}{\partial\Delta^2\partial\omega^2}=\frac{f^2M}{2\pi}\frac{K(\Delta^2)\sigma(\omega)}{p_i^2\mu^2}\times[\omega^4-2\omega^2(M^2+\mu^2)+(M^2-\mu^2)^2]^{1/2}, \tag{14}$$

where $f^2=0.08$ is the renormalized pion nucleon coupling constant, M is the nucleon mass, p_i is the laboratory momentum of the incident proton, and $\sigma(\omega)$ is the π^+-p cross section at an energy ω. The quantity in square brackets is just ω^2 times the relativistic three-body phase-space factor, apart from normalization constants.

$K(\Delta^2)$ has a sharp maximum at low Δ^2 which will be reflected in the laboratory energy spectrum of the "spectator" nucleon. This peak, first predicted by Bonsignori and Selleri,[26] was obtained in the results of Batson *et al.*[5,25] and is clearly in evidence in the present experiment. Figures 9(a), (b), and (c) show the laboratory energy spectra of nucleons from the $pn\pi^+$ and $pp\pi^0$ reactions. The sharpest low-energy peak is in (a) because of the dominance of the π^+-p cross section; this

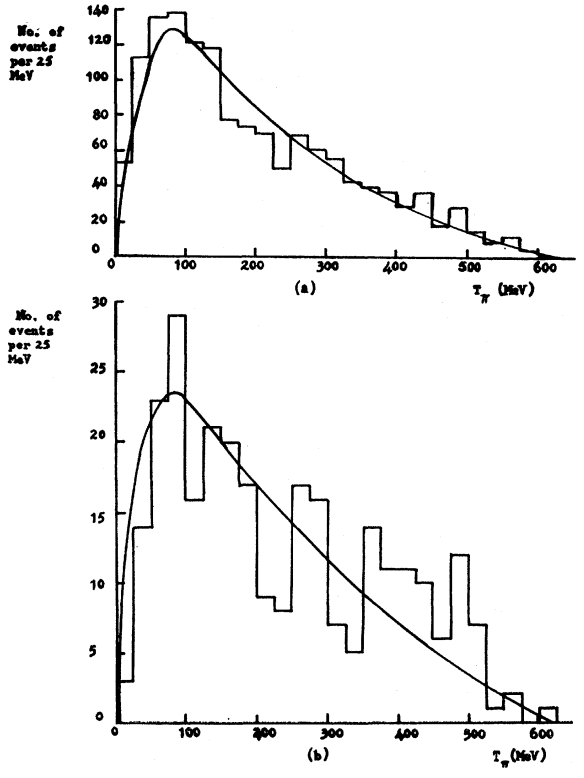

FIG. 10. Laboratory energy spectra of pions from (a) $p+p \rightarrow p+n+\pi^+$, and (b) $p+p \rightarrow p+p+\pi^0$. The solid curves are phase-space predictions normalized to the total number of events.

[25] F. Selleri, Phys. Rev. Letters **6**, 64 (1961). His expression for the cross section is too small by a factor of 2.

[26] F. Bonsignori and F. Selleri, Nuovo Cimento **15**, 465 (1960).

peak is produced by the proton at rest in the laboratory acting as spectator, whereas the high-energy one arises from the incident proton acting as spectator. In the former case, Δ^2 is equal to $2MT$, where T is the laboratory kinetic energy acquired by the spectator nucleon.

The cross sections predicted by the Feynman graphs of Fig. 7 have been calculated, including interference terms, by Da Prato[24] and by Ferrari and Selleri,[24] using the partial-wave amplitude for the $T=J=\frac{3}{2}$ resonant state only. They are shown as dashed and dotted lines, respectively, in Figs. 9(a), (b), and (c). The calculations are absolute ones and, like the result in Eq. (14), depend only on the pion-nucleon coupling constant, the π-p cross sections, and kinematic factors. The agreement with experiment at low momentum transfers is, therefore, strong evidence in favor of the peripheral model. No comparable "spectator" effects are observed in Figs. 10(a) and (b), which show the kinetic energy spectra of pions in the laboratory system. The theoretical curves differ because those of Ferrari and Selleri include a pionic form factor for the nucleon. They had noted[27] that the laboratory energy spectra of nucleons

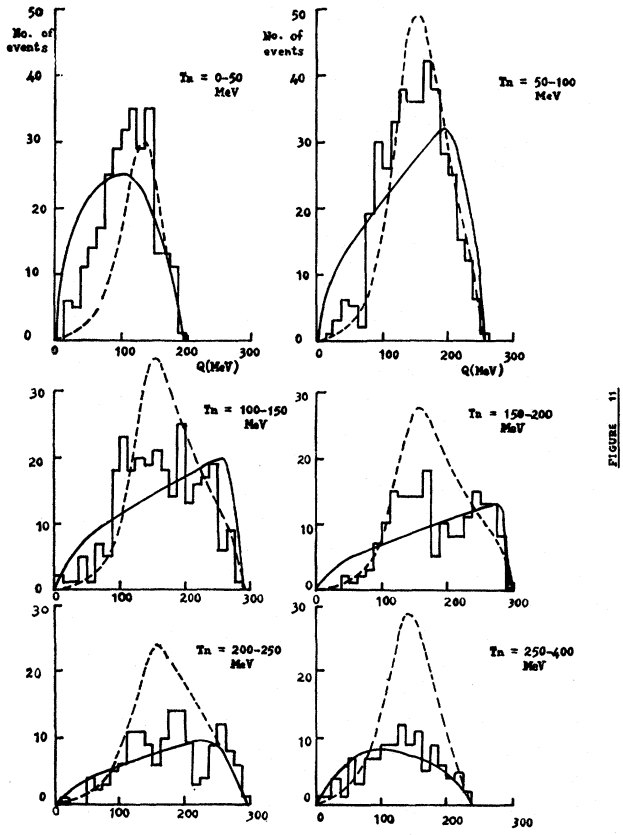

FIGURE 11

FIG. 11. Q-value distributions of π^+p pairs from $p+p\rightarrow p+n+\pi^+$ in six intervals of momentum transfer to the neutron. The solid curves are phase-space predictions normalized to the number of events in each interval, and the dashed curves are the predictions of the peripheral model (Ref. 25) without the pionic form factor.

[27] E. Ferrari and F. Selleri, Phys. Rev. Letters **7**, 387 (1961).

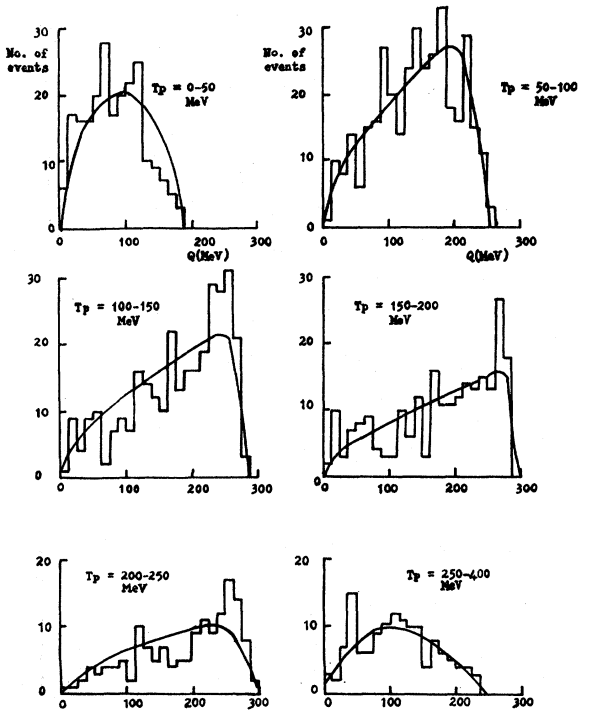

FIG. 12. Q-value distributions of π^+n pairs from $p+p\rightarrow p+n+\pi^+$ in six intervals of momentum transfer to the proton. The solid curves are phase-space predictions normalized to the number of events in each interval.

both at 970 MeV and at 2.85 BeV[28] show less events with large momentum transfers than predicted by the one-pion exchange diagrams of Fig. 7. Assuming all diagrams other than one-pion exchange to be negligible, they have achieved[24,27] impressive agreement with all the nucleon laboratory energy spectra at 970 MeV, 2 BeV,[1] and 2.85 BeV, using a single empirical form factor. Although this form factor is no doubt qualitatively correct, it should be remembered that the theory takes no account of (nonperipheral) Feynman graphs well away from the one-pion pole.

The identity of the protons in the initial state makes all distributions symmetrical forward and backward in the center-of-mass system, and use may be made of the symmetry by folding together both hemispheres in the center-of-mass system. In the laboratory system this amounts to folding about the line

$$T=(1/4M)[M^2+2MT_i-\omega^2],$$

where T_i is the laboratory kinetic energy of the incident proton. In practice, the folding may be done by taking as spectator that initial nucleon which would produce the smaller value of Δ^2 in turning into the neutron. Using all the data in this way, the region of validity of the peripheral model and the $(\frac{3}{2},\frac{3}{2})$ resonance is tested in Fig. 11, which shows the Q-value distribution of π^+p

[28] G. A. Smith, H. Courant, E. C. Fowler, H. Kraybill, J. Sandweiss, and H. Taft, Phys. Rev. **123**, 2160 (1961).

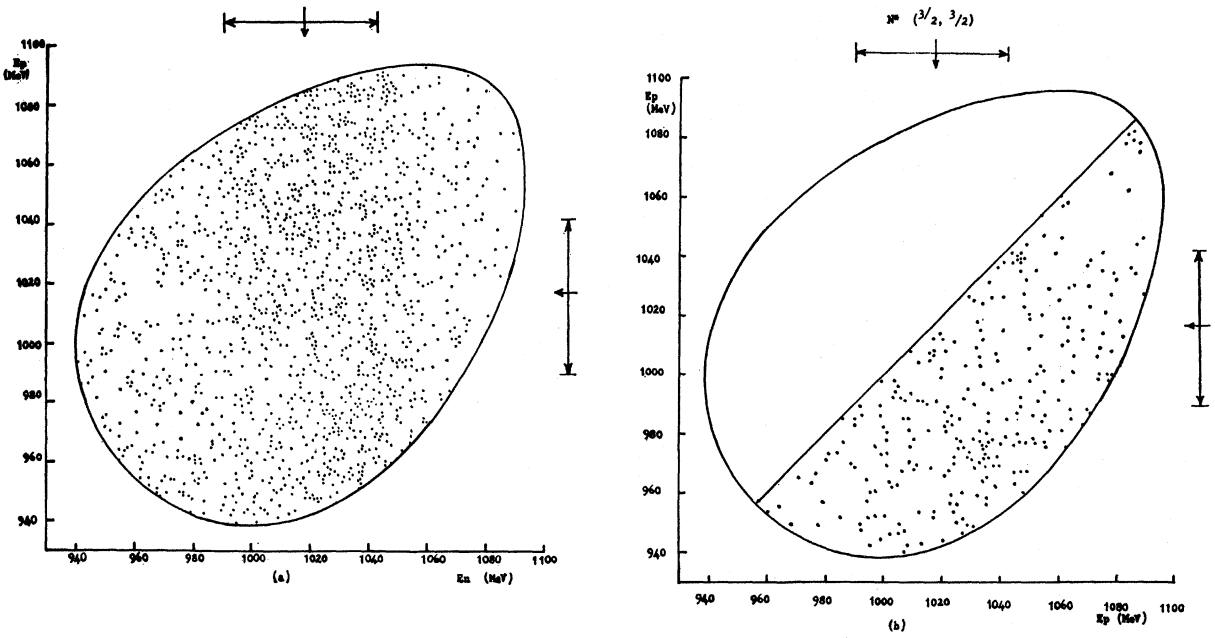

FIG. 13. The Dalitz plots for (a) $p+p \rightarrow p+n+\pi^+$ and (b) $p+p \rightarrow p+p+\pi^0$. E_p and E_n are the center-of-mass energies of proton and neutron. The arrows show the positions of the $(\frac{3}{2},\frac{3}{2})$ resonance and its half-width.

pairs as a function of the neutron kinetic energy. At lower momentum transfers, the $(\frac{3}{2},\frac{3}{2})$ resonance is clearly in evidence, and quantitative agreement with the predictions of Selleri[25] is good. At larger momentum transfers, the effects of the resonance appear to diminish, the experimental results agreeing better with the phase space curves. The theoretical curves do not however include the pion form factor. Figure 12 shows the corresponding results for π^+n pairs; the effects of the resonance are absent, and the predictions of the statistical model fit the results quite closely.

Dalitz plots for both inelastic reactions are shown in Figs. 13(a) and (b). On the basis of phase space alone, events should be uniformly distributed over the plot; that is, the phase space is proportional to dE_1dE_2, where E_1 and E_2 are the center-of-mass energies of the nucleons. The $(\frac{3}{2},\frac{3}{2})$ resonance in the π^+p state produces a broad band of events around $E_n=1017$ MeV on Fig. 13(a), but there is no sign of the same resonance in the π^+n state, even at the sides of the plot where the effect of the π^+p resonance would be small; no interference effect is evident where the resonances would cross. Events are rather sparse on Fig. 13(b), but there is some concentration of events around energies corresponding to the resonance in the π^0p state.

TABLE II. Values of T_p, the laboratory kinetic energy of the proton in the $pn\pi^+$ final state, as a function of $\Delta^2/2M$, the Q value of the $p\pi^+$ pair, and $\cos\theta$. All energies are in MeV.

$\Delta^2/2M$ (MeV)	Q (MeV) \ $\cos\theta$	1.0	0.8	0.4	0	−0.4	−0.8	−1.0
50	100	16	29	55	81	108	134	147
	150	11	29	65	101	136	172	190
	200	8	31	77	123	168	214	237
100	100	37	54	88	122	156	189	206
	150	28	51	95	140	185	229	251
	200	22	50	105	161	216	272	300
150	100	62	82	122	162	203	243	263
	150	48	75	127	179	231	284	310
	200	39	71	135	199	263	327	359

Among those peripheral events in which the π^+p pair emerge with a Q value close to the resonance energy, one would expect to observe the $(1+3\cos^2\theta)$ angular distribution, which is characteristic of the $(\frac{3}{2},\frac{3}{2})$ resonance, for the pion scattering angle in the π^+p rest system. Figure 14(a) shows those events with Q within 50 MeV of the resonance energy and $\Delta^2/2M$ <150 MeV; there is a noticeable forward peak, but little backward peaking. Corresponding results for $Q<100$ MeV and $Q>200$ MeV are shown in Figs. 14(b) and (c). Ideally, the angular distribution should be determined over a range of T values and extrapolated to the pole at $T=-\mu^2/2M$, but in this experiment, as in similar results at 2.0 BeV published in a letter by Fickinger *et al.*[1] there are insufficient events to carry out such a procedure. Within our limited statistics, the results for $\Delta^2/2M<100$ MeV and $\Delta^2/2M<50$ MeV are the same as those in Fig. 14.

The reason for the discrepancy between the observed angular distribution and $(1+3\cos^2\theta)$ is not clear, although some isotropic background reducing the forward and backward peaks would hardly have been surprising. Indeed, in the case of free π^+-p scattering, both the small phase shifts δ_3 and δ_{31} are of the order of $-10°$ with the result that the angular distribution is close to $(2.5\cos^2\theta+1)$. An effect around $\cos\theta=0$ due to overlapping of the π^+p and π^+n resonances might have been expected also, but is not present. The forward peak

in the angular distribution corresponds to some concentration of events near the upper phase-space boundary of the Dalitz plot around $E_n=1017$ MeV; the absence of a backward peak, which should appear near the lower phase-space boundary, cannot be explained as an interference between π^+p and π^+n resonances.

Ferrari and Selleri[29] have investigated the behavior of the π^+-p scattering amplitude off the mass shell using dispersion relations, and taking only the $(\frac{3}{2},\frac{3}{2})$ amplitude to be important. Their result is that, off the mass shell, the magnitude of the amplitude is somewhat affected by kinematic factors, but the $(1+3\cos^2\theta)$ form of the angular distribution is preserved, as might be expected since $\cos\theta$ is a variable independent of ω and Δ^2.

However, $\cos\theta$ is related to the four-momentum

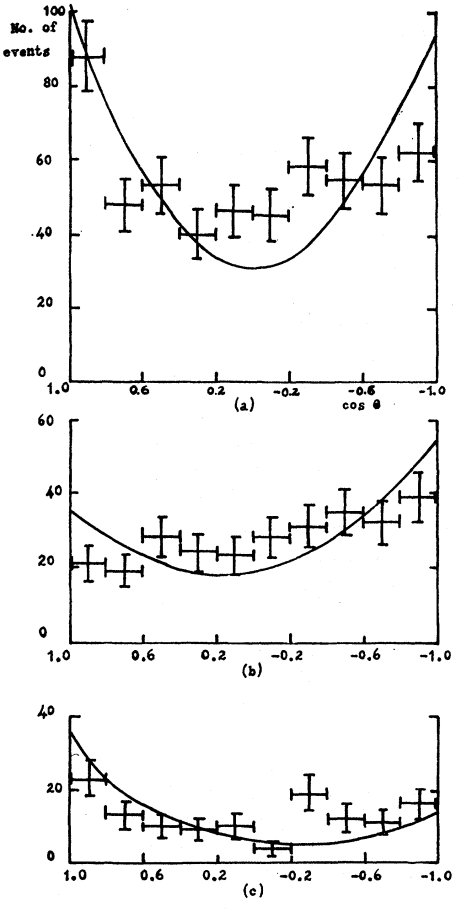

FIG. 14. The π^+-p angular distribution in the π^+p rest frame, for those events in which $\Delta^2/2M<150$ MeV and (a) $100<Q<200$ MeV, (b) $Q<100$ MeV, and (c) $Q>200$ MeV. The solid curves are the predictions of the peripheral model, including the pionic form factor (Ref. 24). They are normalized to the number of events in each interval.

[29] E. Ferrari and F. Selleri, Nuovo Cimento **21**, 1028 (1961); also O. Iizuka and A. Klein, Progr. Theoret. Phys. (Kyoto) **25**, 1018 (1961).

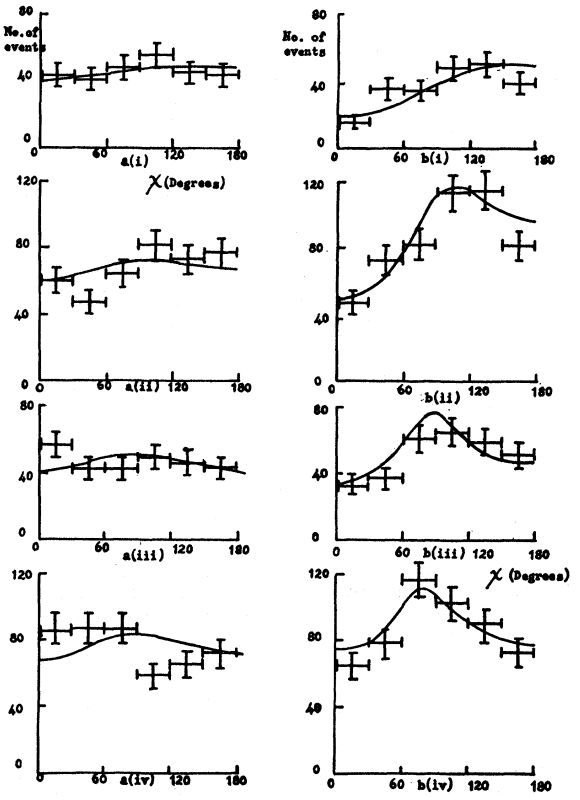

FIG. 15. The Treiman-Yang test applied to the $p+p\rightarrow n+p+\pi^+$ reaction taking (a) the neutron, and (b) the proton as the spectator particle: (i) $T<50$ MeV; (ii) $50<T<100$ MeV; (iii) $100<T<150$ MeV; and (iv) $T>150$ MeV. The solid curves show the predictions of the one-pion exchange model, including the pionic form factor (Ref. 24), normalized to the number of events in each interval.

transfer (t) to the proton of the final state. Specifically,

$$t^2=(p_1-q_1)^2=2MT_p=2q_{10}p_{10}-2q_1p_1\cos\theta-2M^2, \quad (15)$$

where the proton of the final state has energy q_{10} and momentum q_1 in the π^+p rest system, and kinetic energy T_p in the laboratory system, and the "nonspectator" proton of the initial state has energy p_{10} and momentum p_1 in the π^+p rest system. The quantities q_{10}, q_1, p_{10}, and p_1 depend only on ω and Δ^2, and Table II shows T_p as a function of $\cos\theta$ and Δ^2 for various Q values of the π^+p system. This table indicates that the absence of a backward peak in Fig. 14 corresponds to the sharp drop at 150 MeV in Fig. 9(b), the laboratory energy spectrum of protons from the $pn\pi^+$ reaction. Ferrari and Selleri explained this drop at intermediate t values in part by attributing a form factor to the exchange pion; but since the amplitude for π^+ exchange [Figs. 7(a) and (b)] is three times as great as for π^0 exchange [Figs. (c) and (d)], such a factor affects Fig. 9(b) largely through Δ^2-dependent factors, and the expected angular distributions in Fig. 14 ought to be little affected by such factors. Calculation of the angular distribution from the formulas of Ref. 24 including the pion form

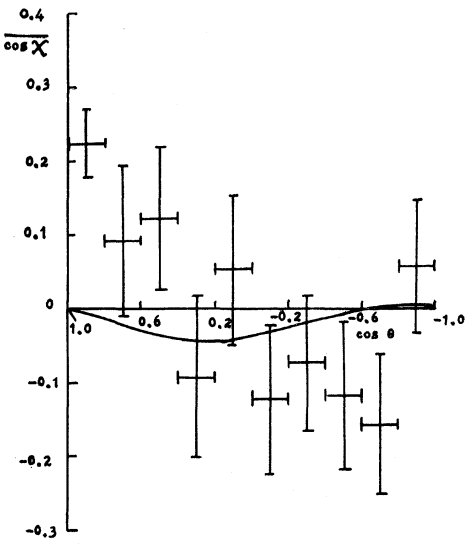

FIG. 16. The average value of $\cos\chi$ as a function of $\cos\theta$ for $T<150$ MeV and ω within 50 MeV of the resonance. The solid curve shows the prediction of the one-pion exchange model, including the pionic form factor (Ref. 24).

factor confirms this, and gives the curves shown on Fig. 14.

It is concluded, therefore, that the absence of a backward peak in Fig. 14 and the drop in Fig. 9(b) at $T_p=150$ MeV are probably due to some phenomenon other than the pion form factor of Ferrari and Selleri. Attention is drawn to the fact that the connection between $\cos\theta$ and t through Eq. (15) may affect the determination of the angular momentum of an isobaric state produced in peripheral inelastic reactions, unless attention is confined to the lowest possible values of Δ^2.

A critical test of the peripheral model follows from the fact that the exchanged pion has spin zero. As Treiman and Yang[30] have pointed out, this implies that the π^+p pairs should show no azimuthal asymmetry around the direction of the virtual pion, that is, in the angle χ of Fig. 8. The results of this test are given in Fig. 15(a) for various ranges of momentum transfer to the neutron. No asymmetries are observed which could not reasonably be attributed to statistical fluctuations. However, if, instead, the proton is taken to be the spectator, the results shown in Fig. 15(b) are obtained. In this case there is a reduction in the number of events towards $\chi=0°$, which can be traced to the strong tendency to association between the proton and the π^+. Ferrari[31] has pointed out that such an asymmetry arises from interference between the diagrams of Figs. 7. Using the formulas of Ref. 24, the solid curves shown on Figs. 15(a) and (b) have been calculated, and are in good accord with experiment.

[30] S. B. Treiman and C. N. Yang, Phys. Rev. Letters **8**, 140 (1962).
[31] E. Ferrari, Phys. Letters **2**, 66 (1962).

However, Fig. 15(a), in particular, is a little misleading. For given Δ, ω, and θ, the Q value of the π^+n system will depend on the angle χ between the qq_1 and q_2p_2 planes and, therefore, interference effects between π^+p and π^+n resonances should be revealed as an asymmetry in χ as a function of θ for given Δ and ω, particularly near $\cos\theta=0$, where the resonances overlap. The average value of $\cos\chi$ has been determined as a function of $\cos\theta$ for $T_n<150$ MeV and ω within 50 MeV of the resonance, and is shown in Fig. 16. There are some signs of asymmetries, but they are not restricted to the region of overlapping resonances. The solid curve of Fig. 16 is calculated from the formulas of Ref. 24; in spite of the limited statistical accuracy, it appears that neither the signs nor the magnitudes of the asymmetries are correctly predicted. The observed asymmetries may be understood qualitatively as a tendency for π^+ and n to go off together, particularly for large π^+-p scattering angles. However, the magnitude of the effect, which is largest near $\cos\theta=\pm1$, where interference effects between π^+p and π^+n isobars would be expected to be small, is not easy to understand. It indicates that there are probably contributions to the $pn\pi^+$ reaction from mechanisms other than single-pion exchange.

Because of the success of the peripheral model, a search was made for an asymmetry of the proton from the π^+-p vertex about the spin direction of the incident proton. With statistics similar to those in Fig. 4(a), no asymmetry was found at any interval of θ in the range 0–180°.

The center-of-mass angular distributions of particles from the inelastic collisions are shown in Figs. 17(a)–(e). They are symmetrical forward and backward within statistical errors, indicating that there has not been any substantial scanning loss or misidentification of events. As expected from the peripheral model, the nucleon angular distributions are strongly peaked near 0° and 180°, the neutrons somewhat more than the protons in the $pn\pi^+$ reaction. The pions in this reaction also peak forward and backward. Center-of-mass angular correlations between pairs of particles, drawn in Figs. 18(a)–(e), show no unexpected features. Nucleon-nucleon correlations are strongly peaked near 180°, indeed, to rather a larger extent than predicted by phase-space calculations. This is again due to the peripheral mechanism, which causes the strong forward-backward peaking in Figs. 17. Center-of-mass momentum spectra of nucleons are not given here, since they simply reflect the Q-value distributions of π-nucleon pairs. Center-of-mass pion spectra, however, are drawn in Figs. 19(a) and (b).

Any spin-dependent effects in inelastic interactions would contribute to the scattering through terms of the form $\boldsymbol{\sigma}\cdot\mathbf{k}_{\rm inc}\times\mathbf{k}_1$, $\boldsymbol{\sigma}\cdot\mathbf{k}_{\rm inc}\times\mathbf{k}_2$, or $\boldsymbol{\sigma}\cdot\mathbf{k}_1\times\mathbf{k}_2$, where $\boldsymbol{\sigma}$ and $\mathbf{k}_{\rm inc}$ are the spin and momentum vectors of the incident proton, and $\mathbf{k}_1$ and $\mathbf{k}_2$ are the momentum vectors of any two particles in the final state. That is, there should

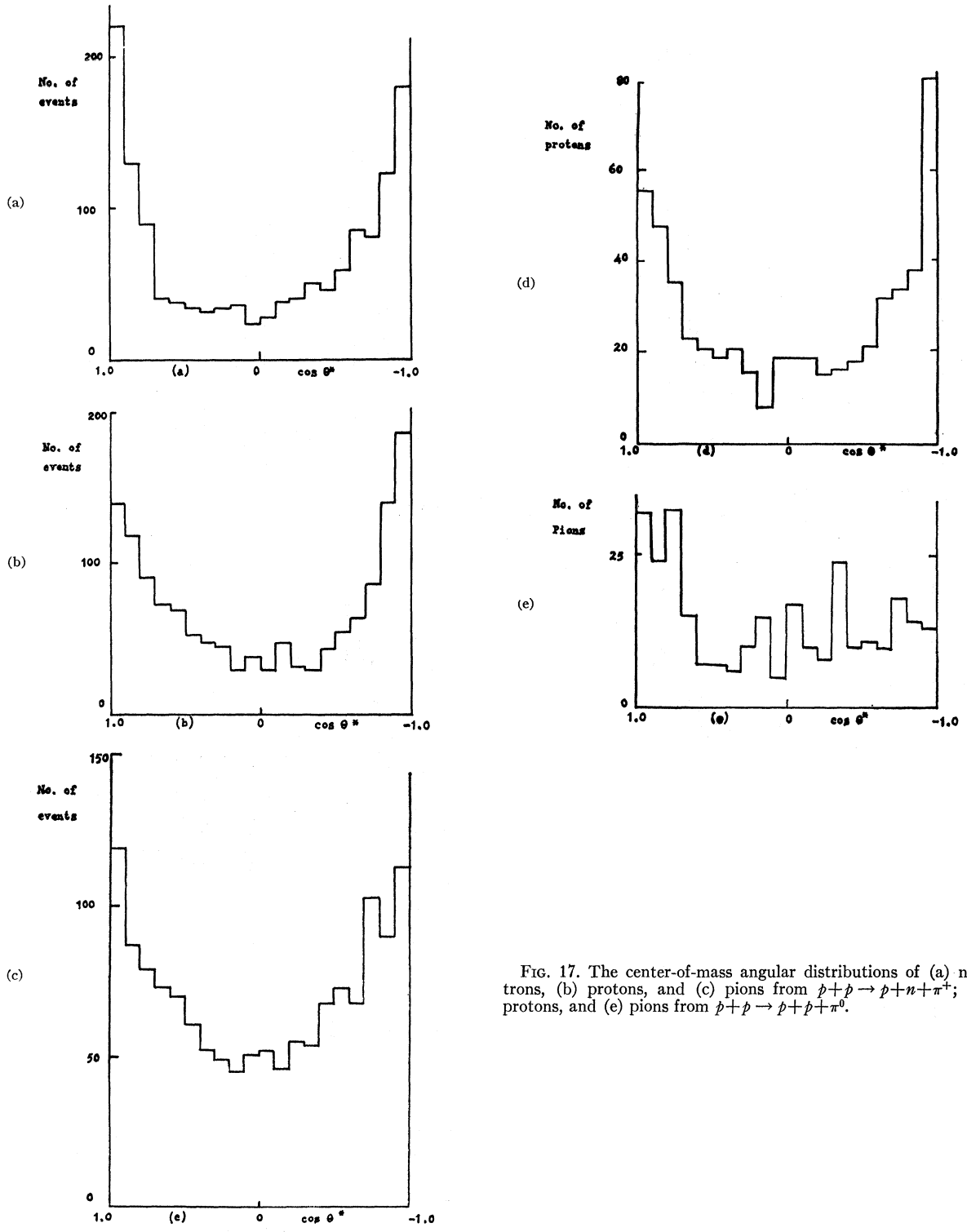

FIG. 17. The center-of-mass angular distributions of (a) neutrons, (b) protons, and (c) pions from $p+p \rightarrow p+n+\pi^+$; (d) protons, and (e) pions from $p+p \rightarrow p+p+\pi^0$.

appear left-right asymmetries in the proton or neutron angular distributions, or azimuthal asymmetries of the proton-neutron plane. A careful search has been made for any such effect, but none has been observed which is statistically significant. As an example, the average values of the first two quantities above are plotted against the center-of-mass scattering angle in Fig. 20; no significant asymmetries are observed.

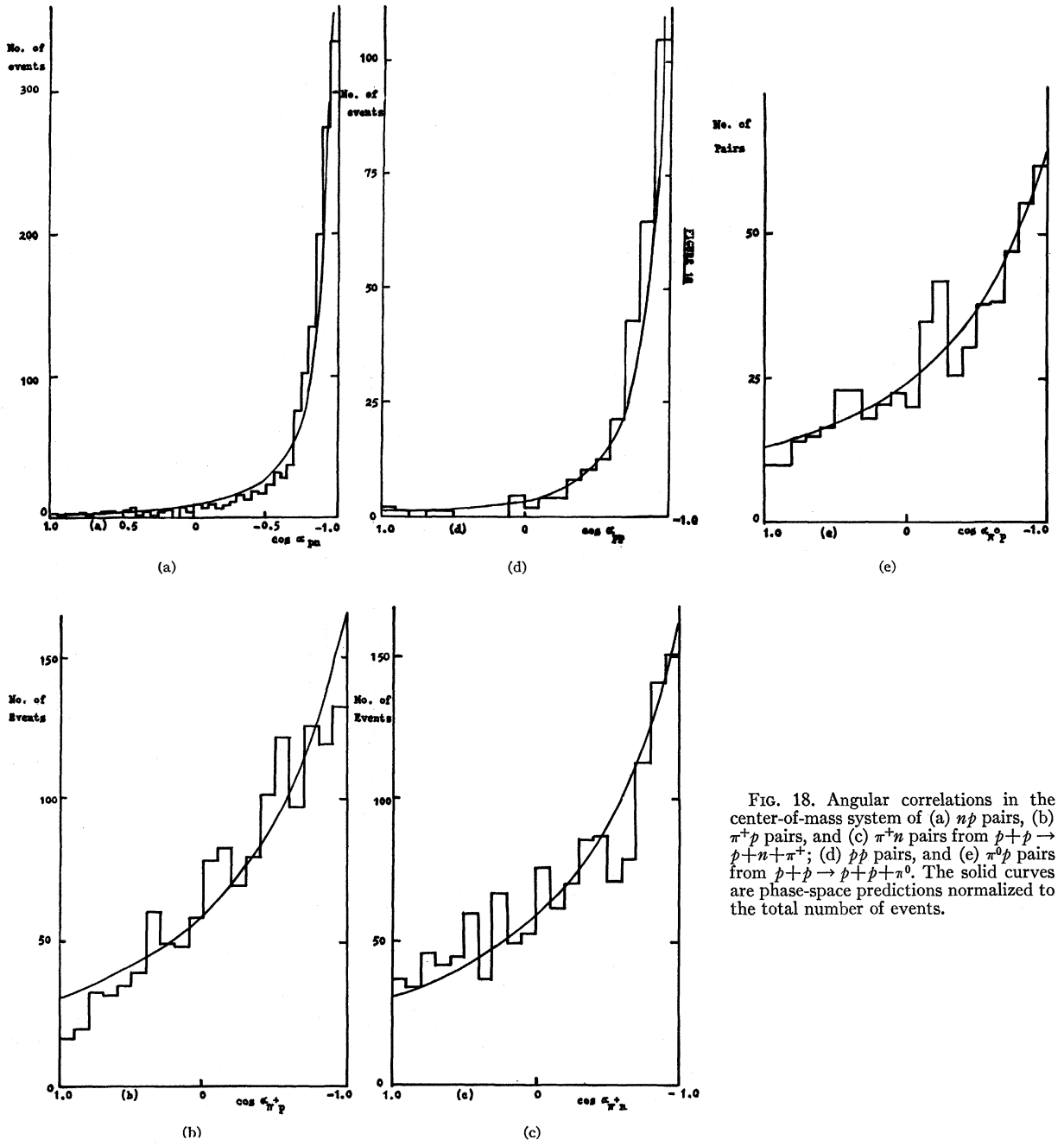

FIG. 18. Angular correlations in the center-of-mass system of (a) np pairs, (b) π^+p pairs, and (c) π^+n pairs from $p+p \rightarrow p+n+\pi^+$; (d) pp pairs, and (e) π^0p pairs from $p+p \rightarrow p+p+\pi^0$. The solid curves are phase-space predictions normalized to the total number of events.

Several checks on parity conservation are possible in this experiment, and all have been found to be satisfied within experimental error. For example, in the Treiman-Yang test, χ should be symmetric about 0°; that is, there should be no asymmetries of the form $(\mathbf{p}_2-\mathbf{q}_2)\times(\mathbf{p}_2\times\mathbf{q}_2)\cdot(\mathbf{q}\times\mathbf{q}_1)$.

This test was well satisfied, as were those in which the identities of the particles in the final state were permuted. Since the incident beam is polarized, parity nonconservation might lead to up-down asymmetries of the form $\boldsymbol{\sigma}\cdot\mathbf{k}$ in elastic or inelastic scattering, $\mathbf{k}$ being a unit vector in the direction of any final-state particle; no statistically significant asymmetries have been observed.

8. CONCLUSIONS

A detailed study of p-p scattering has been made at an incident energy of 970 MeV. The cross section for elastic scattering agrees with the counter result of McFarlane *et al.*,[14] but is higher than the counter result of Dowell *et al.*,[13] although the shape of the angular

distribution agrees well with their result. Observations of polarization effects in elastic scattering are consistent with a previous and more accurate experiment of Homer *et al.*[12,16] The shape of the polarization curve appears to demand sizeable contributions from angular momentum states up to $l=5$, indicating quite a long-range spin-dependent nucleon potential.

Many features of the inelastic reactions, for the $pn\pi^+$ final state, in particular, are in good agreement with the peripheral model especially at low momentum transfers (Figs. 9 and 11). Against this must be balanced (a) the disagreement between the π^+-p center-of-mass angular distribution and the expected $(1+3\cos^2\theta)$, and (b) the indication from the restricted Treiman-Yang test of Fig. 16 that there may be contributions from graphs other than single-pion exchange. It is difficult to see why cross sections agree so well with single-pion exchange when the angular distributions are not so good. Since the exchanged pion of Fig. 8 is virtual and the discrepancies with the model arise only in angular distributions, it is tempting to suppose that the exchanged pion is behaving as a Regge pole, and is acquiring nonzero spin off the mass shell. Such speculation would, however, not appear to be in accord with the fact that Ferrari and Selleri have been able to fit the laboratory energy spectra of nucleons at both 970 MeV and 2.85 BeV with the same pion form factor.

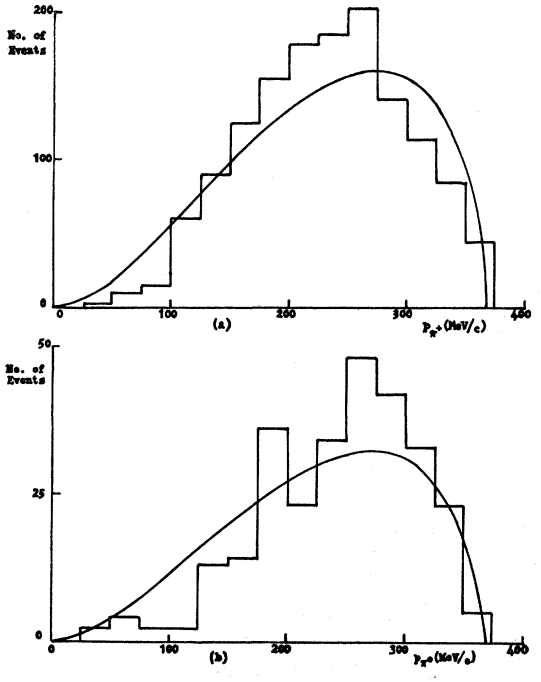

FIG. 19. Center-of-mass momentum spectra of pions from (a) the $pn\pi^+$ final state, and (b) the $pp\pi^0$ final state. The solid curves are phase-space predictions normalized to the total number of events.

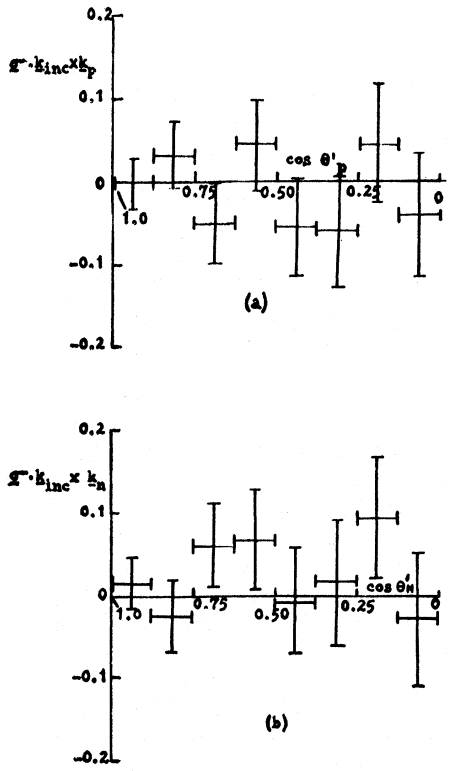

FIG. 20. The average values, as functions of the center-of-mass scattering angle, θ', of (a) $\boldsymbol{\sigma}\cdot\mathbf{k}_{\rm inc}\times\mathbf{k}_p$, and (b) $\boldsymbol{\sigma}\cdot\mathbf{k}_{\rm inc}\times\mathbf{k}_n$, in the $pn\pi^+$ final state. The results are folded about $\cos\theta'=0$.

ACKNOWLEDGMENTS

The success of the experiment depended on many other people, to whom we are most grateful. In particular, we wish to acknowledge the support of the operating staffs of the Birmingham University proton synchrotron, of Edsac 2 at Cambridge, and of the Ferranti Mercury computer at Manchester. R. Marsh at Cambridge and C. Barrow at Birmingham provided invaluable technical assistance. We are grateful to Dr. E. Ferrari and Dr. F. Selleri of CERN, L. Castillejo and Professor S. Mandelstam at Birmingham for theoretical guidance, and Professor O. R. Frisch and Professor P. B. Moon for their interest and support. Most of the scanning and measurement was done by our several female assistants, to whom we are greatly indebted. Part of the cost of the work was provided by the D.S.I.R.